

1 *STH-net*: a soil monitoring network for process-based hydrological 2 modelling from the pedon to the hillslope scale

3 Edoardo Martini^{1,2}, Matteo Bauckholt², Simon Kögler^a, Manuel Kreck², Kurt Roth¹, Ulrike Werban², Ute
4 Wollschläger³, Steffen Zacharias²

5 ¹ Institute of Environmental Physics, Heidelberg University, Heidelberg, 69120, Germany

6 ² Dept. Monitoring and Exploration Technologies, Helmholtz Centre for Environmental Research GmbH - UFZ, Leipzig,
7 04318, Germany

8 ^a formerly at: Dept. Monitoring and Exploration Technologies, Helmholtz Centre for Environmental Research GmbH - UFZ,
9 Leipzig, 04318, Germany

10 ³ Dept. Soil System Science, Helmholtz Centre for Environmental Research GmbH - UFZ, Halle (Saale), 06120, Germany

11 *Correspondence to:* Edoardo Martini (emartini@iup.uni-heidelberg.de)

12 **Abstract.** The *Schäfertal hillslope* site is part of the TERENO Harz/Central German Lowland Observatory and its soil water
13 dynamics are being monitored intensively as part of an integrated, long-term, multi-scale and multi-temporal research
14 framework linking hydrological, pedological, atmospheric and biodiversity-related research to investigate the influences of
15 climate and land use change on the terrestrial system. Here, a new soil monitoring network, indicated as *STH-net*, has been
16 recently implemented to provide high-resolution data about the most relevant hydrological variables and local soil properties.
17 The monitoring network is spatially optimized, based on previous knowledge from soil mapping and soil moisture monitoring,
18 in order to capture the spatial variability of soil properties and soil water dynamics along a catena across the site as well as in
19 depth. The *STH-net* comprises eight stations instrumented with time-domain reflectometry (TDR) probes, soil temperature
20 probes and monitoring wells. Furthermore, a weather station provides data about the meteorological variables. A detailed soil
21 characterization exists for locations where the TDR probes are installed. All data are measured at a 10-minutes interval since
22 January 1st, 2019. The *STH-net* is intended to provide scientists with data needed for developing and testing modelling
23 approaches in the context of vadose-zone hydrology at spatial scales ranging from the pedon to the hillslope. The data are
24 available from the EUDAT portal (<https://b2share.eudat.eu/records/82818db7be054f5eb921d386a0bcaa74>) (Martini et al.,
25 2020).

26 **1 Introduction**

27 Soils are embedded in the environment, coupled to vegetation and atmosphere at the land surface and to groundwater at its
28 lower end. This coupling gives rise to a suite of physical, chemical, and biological dynamics most of which are highly non-
29 linear and varying in time and space. Soils provide crucial ecosystem functions such as water storage and filtering, food and
30 other biomass production, recycling of carbon and nutrients, biological habitat and gene pool, physical and cultural heritage,
31 source of raw materials and platforms for human life (United Nations, 2014; Vereecken et al., 2016). Soils are widely
32 distributed on the Earth surface. Flow and transport processes in unsaturated soils occur predominantly in the vertical direction,
33 with the gravity force playing a major role, as abrupt changes in soil properties due to soil horizons and layers are typically

34 more significant than those in the lateral direction, and because of the strong coupling between soil, vegetation, and
35 atmosphere. Therefore, despite the relevance of soils for global phenomena, the relevant soil processes are rather local. Here,
36 one aspect that complicates the picture is the heterogeneity of soil properties. Another one is the non-linearity of soil processes.
37 In order to address effectively this complexity, state-of-the-art experimental approaches must be coupled to numerical models
38 for the comprehensive representation of the system properties, states and fluxes so that the hydrological system can be better
39 understood.

40 Recently, Vogel (2019) provided a comprehensive discussion about the scales and scaling issues in the context of soil
41 hydrological research and noted the need for looking at small-scale soil properties (i.e., at the pedon scale, at which soil physics
42 is capable of describing states and fluxes with sufficient accuracy) as a necessary step towards understanding and summarizing
43 the processes at larger scales. In this respect, the author stresses the need for a two-steps approach based on the accurate
44 description of the soil water dynamics at the pedon scale and accounting for the spatial patterns of functional soil types that
45 constitute the landscape, including the vertical stratification of soil hydraulic properties and structural attributes. However, the
46 author remarks that high-resolution measurements of the relevant states and properties cannot be achieved at the larger scale
47 (i.e., catchment, the typical scale of application of hydrological research). In this context, the intermediate scale of hillslopes
48 is crucial for linking the detailed process understanding to larger scale dynamics, recognizing hillslopes as key landscape
49 features that organize water availability on land (Fan et al., 2019). In this respect, coupling state of the art hydrological
50 modelling approaches with high-resolution subsurface characterization can lead to an accurate quantification of the soil water
51 dynamics in the vadose zone (Vereecken et al., 2015).

52 The physical description of the small-scale water movement through the soil's porous structure is typically achieved using the
53 Richards equation. However, the detailed description of the material properties is needed and cannot be fully resolved by direct
54 sampling. Thus, inverse modelling can be a powerful tool for the estimation of the soil hydraulic parameters (e.g., Vrugt et al.,
55 2008), including the recent developments in data assimilation approaches (e.g., Bauser et al., 2016, 2020; Botto et al., 2018).
56 These require dense (in the direction of the dominant flow, typically orthogonal to the soil surface) measurements of soil water
57 content with high temporal resolution and of high quality. Furthermore, *in situ* sensors can experience all the processes
58 affecting the measured state variables in their natural environment (Wollschläger et al., 2009), which is an important advantage
59 with respect to sample-based determinations from the laboratory.

60 The performances of hydrological models can be improved by various measured data with high spatial and temporal resolution
61 (Clark et al., 2017). Bronstert (1999) highlighted the importance of linking experimental knowledge to the experience gained
62 from numerical modelling applications as a very valuable synergistic combination. Technological advances in our ability to
63 measure soil hydrological states efficiently at the hillslope scale and beyond are one possible way to gain the much-needed
64 improved understanding of processes that challenge the comprehensive understanding of field-scale hydrology.

65 In the research framework of the TERENO Harz/Central German Lowland Observatory, the *Schäfertal hillslope* represents a
66 benchmark site for developing and testing the integration of state-of-the-art monitoring techniques with advanced modelling
67 approaches. This offers the opportunity to gain a more detailed understanding of processes and to quantify and predict water

68 and matter fluxes at nested spatial scales in the context of climate and land use change. Specifically, the approach followed at
69 the site accounts for the soil spatial variability through detailed soil mapping and is designed to provide *in situ* data with high
70 temporal resolution and dense coverage in the vertical direction, about the soil water dynamics in the vadose zone and of its
71 boundary conditions. With this design tailored to the needs of vadose zone modelling, we aim to provide physical models with
72 ideally all the data needed for quantifying and predicting the soil water fluxes at spatial scales ranging from the pedon to the
73 hillslope scale, with important implications, in terms of methodological advance and process understanding, for catchment-
74 scale processes.

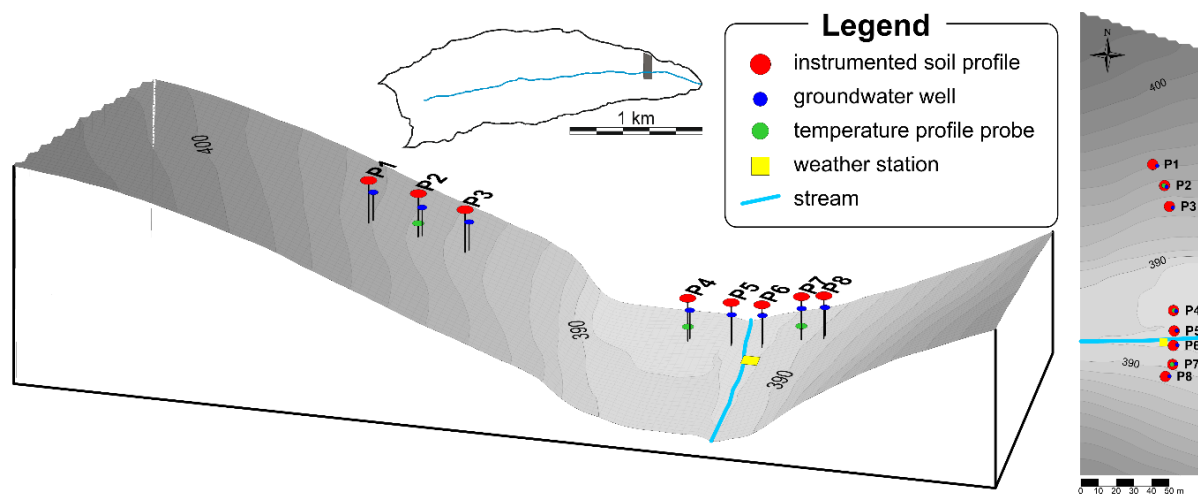
75 Here, we present the first 21 months of the comprehensive dataset measured by the monitoring network *STH-net*, recently
76 implemented at *Schäufertal Hillslope* site, part of an intensive hydrological observatory. The data set includes hourly time series
77 of the meteorological forcing, soil water content measured *in situ* at different locations and at multiple soil depths along a
78 hillslope transect, soil physical and physicochemical properties.

79 **2 Site description**

80 The Schäufertal experimental site is a small headwater catchment (1.44 km²) located in the Lower Harz Mountains, in Central
81 Germany (51°39' N, 11°3' E). Environmental research at the Schäufertal catchment was initiated at the end of the 1960s with
82 the implementation of a hydro-meteorological station (Reinstorf et al., 2010) and the infrastructure has continuously been
83 expanded since then. Since 2010, the Schäufertal catchment is one of the highly instrumented intensive research sites within the
84 TERENO Harz/Central German Lowland Observatory (Zacharias et al., 2011, Wollschläger et al., 2017). Due to the
85 geographical settings of the Harz region, the Schäufertal catchment receives only 630 mm of precipitation per year. The average
86 annual air temperature is 6.9°C, with a sub-continental climate (Reinstorf, 2010). The geology of the catchment is dominated
87 by Devonian argillaceous shales and greywackes, covered by periglacial sediments (Borchardt, 1982). Near-surface compacted
88 horizons within the basal layer are known to induce interflow processes in the unsaturated zone (Borchardt, 1982; Gräff et al.,
89 2009). Dominant soil types in the Schäufertal are Gleysols occurring in the valley bottom as well as Luvisols and Cambisols on
90 the loess-covered slopes (Ollesch et al., 2005). The slopes of the catchment are intensively used for agriculture, whilst meadows
91 occupy the valley bottom (Schröter et al., 2015).

92 Since 2012, a smaller hillslope area named *Schäufertal Hillslope* site, located downstream of the Schäufertal gauging station,
93 was instrumented for detailed investigations of the hydrological processes in the unsaturated zone. From 2012 to 2017, the
94 wireless soil moisture monitoring network *SoilNet* has delivered information about the soil water dynamics at three depths
95 within the unsaturated zone with high spatial coverage. In 2018, the *SoilNet* has been disposed and a new soil monitoring
96 network, named *STH-net*, has been installed aiming to improve the resolution in the vertical direction at a fewer locations
97 selected based on the knowledge about the soil spatial variability and soil water dynamics gained from the previous monitoring
98 experience (see Martini et al., 2015; 2017a; 2017b). The *STH-net* is described in the following sections of this manuscript and
99 its data are now available through the data portal EUDAT

100 (<https://b2share.eudat.eu/records/82818db7be054f5eb921d386a0bcaa74>). The *Schäferfirtal Hillslope* site includes north- and
 101 south-exposed slopes divided by the creek (*Schäferbach*) in the valley bottom (Fig. 1). In contrast to the slopes upstream,
 102 which are primarily covered by cropland, this grassland transect is used as pasture and is not affected by agricultural practices
 103 except that the grass is mowed typically once per year. The spatial extent of the hillslope is approximately 250 by 80 m and
 104 presents various topographical and pedological features. The slopes are covered by silty loam Cambisols more evolved towards
 105 the footslope, while loam and silty loam stagnic Gleysols occupy the valley bottom. An extensive description of the soil units
 106 mapped at the site is provided in Martini et al. (2015). The *STH-net* is designed to cover the spatial variability of the soil
 107 properties as well as the soil layering with high resolution.



108
 109 **Figure 1: Spatial map in 3D and aerial view of the *Schäferfirtal* hillslope site and location of the monitoring stations.**

110 **3 Monitoring design and measurement techniques**

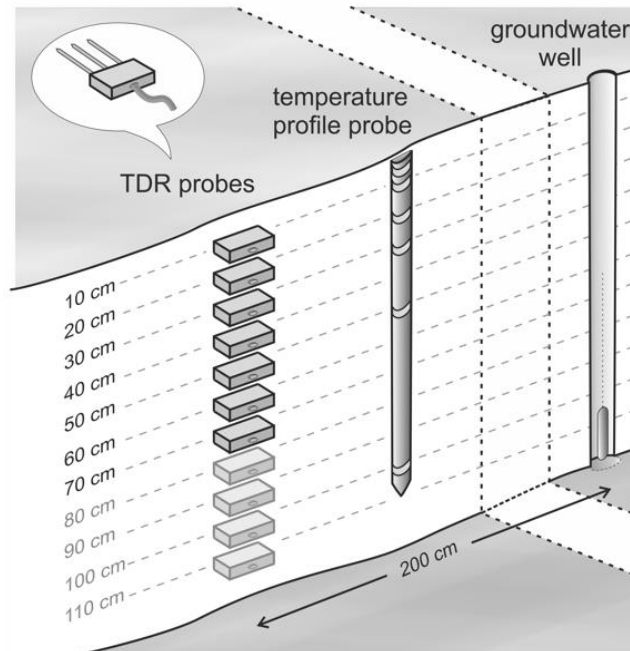
111 The *STH-net* comprises eight monitoring stations (named as P1 to P8) arranged along a transect centred within the *Schäferfirtal*
 112 *Hillslope* site and aligned along the slope direction (Fig.1). The stations P1, P2 and P3 are located within the Northern (i.e.,
 113 South-facing) slope and cover the transition between the soil units STU1 and STU2 described in Martini et al. (2015); the
 114 stations P4 and P5 fall into the valley bottom, i.e., soil unit STU3; P6, P7 and P8 cover the lower part of the Southern (i.e.,
 115 North-facing) slope, i.e., soil unit STU4. Every station features a soil profile instrumented with Time-Domain Reflectometry
 116 (TDR) probes installed every 0.1 m along the vertical direction. A sketch showing the design of a reference monitoring station
 117 is presented in Fig. 2. Each of the instrumented soil profiles located on the hillslopes features a minimum of seven TDR probes
 118 installed at the depths of 0.1, 0.2, 0.3, 0.4, 0.5, 0.6 and 0.7 m, whilst an additional probe is installed at P3 at the depth of 0.8 m
 119 and the profiles at P4 and P5 feature additional TDR probes at the depths of 0.8, 0.9, 1.0 and 1.1 m in order to cover the deeper
 120 soils. In a few cases, the depths of the probes were adjusted to avoid installing the TDR probe at or too close to the boundaries

121 between soil horizons. The exact depth of every TDR probe is reported in the file “STH-net_Soils.txt” and displayed in Fig.
122 3.

123 At every station, a well instrumented with a piezometer was installed ca. 2 m to the East of the instrumented soil profiles for
124 monitoring the water level. One station for every topographic unit (i.e., Northern slope, valley bottom and Southern slope) was
125 further instrumented with sensors measuring the soil temperature at six depths between 0.05 and 1.0 m.

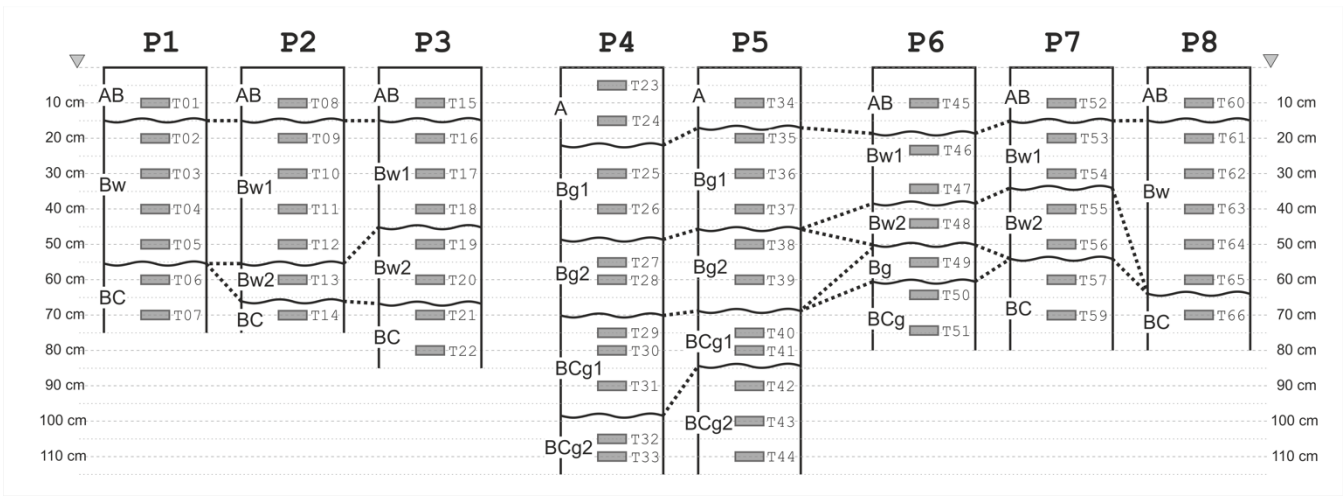
126 A weather station is located in the centre of the hillslope transect next to the creek.

127 All measurement systems comprising the *STH-net* collect measurements every 10 minutes, with the only exception of the
128 water level data which are collected every 2 hours.



129

130 **Figure 2: Sketch of a representative monitoring station of the *STH-net*.**



131

132 **Figure 3: Sketch of the soil profiles (showing the mapped soil horizons according to WRB 2015) and the depth of the TDR probes**
 133 **(see labels).**

134 **3.1 TDR measurements**

135 The TDR probes are arranged in clusters of 22 probes for the Northern slope and the valley bottom, whilst only 21 probes were
 136 installed at the Southern slope, for a total of 65 TDR probes. Each cluster consists of one TDR device (TDR100 for the station
 137 North, TDR200 for the stations Valley and South, Campbell Scientific Inc., Logan, UT, United States) and a data logger
 138 (CR1000 for the station North, CR6 for the stations Valley and South, Campbell Scientific Inc., Logan, UT, United States).
 139 The clusters are powered by extra low voltage cables buried ca. 0.3 m below the ground and cased in HDPE (i.e., high-density
 140 polyethylene) tubes and an AGM (i.e., absorbent glass mat) battery capable of supplying the required power in case of power
 141 cut-off. Every TDR probe is connected to its station master by a 22-m long low loss coaxial cable, tested to be the optimal
 142 length providing good signal quality while enabling enough flexibility in terms of network design. The TDR probes were
 143 custom made and have three 0.2 m-long rods. They were calibrated through measurements in air and in water with different
 144 salt concentrations for water content and electrical conductivity estimation. The probes were installed horizontally in soil pits
 145 which were carefully refilled after the installation. The installation was carried out between June and August 2018 and all the
 146 measurements collected until the end of December 2018 were discarded to allow the soil to re-compact naturally during the
 147 first rainy season.

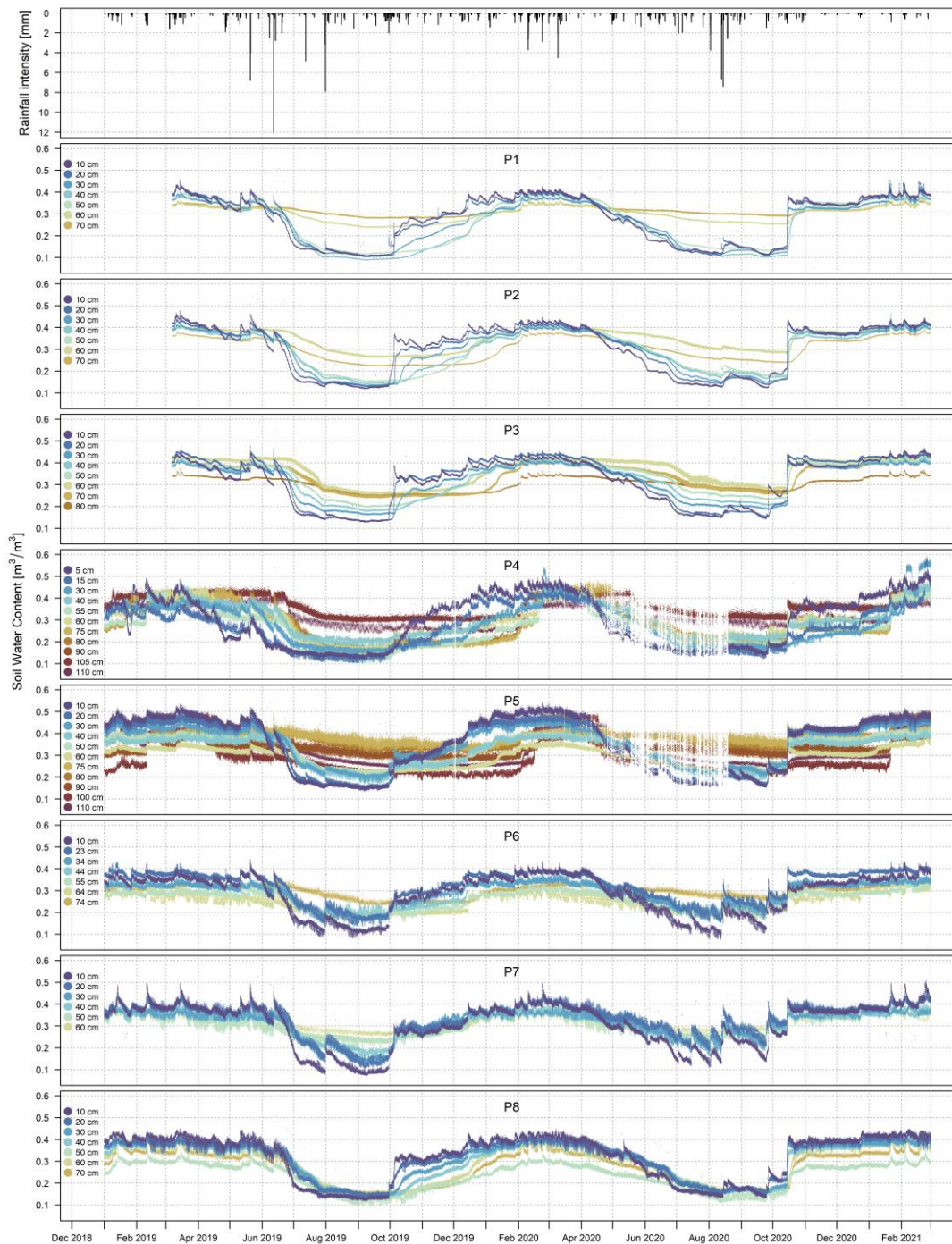
148 From the TDR traces, the dielectric permittivity ϵ of the medium is calculated as:

$$\sqrt{\epsilon} = \frac{(\sqrt{\epsilon_{air}} - \sqrt{\epsilon_{water}})(t - t_{water})}{t_{air} - t_{water}} + \sqrt{\epsilon_{air}} \quad (1)$$

149 based on the calibration measurements of travel time and dielectric permittivity in air (t_{air} , ϵ_{air}) and water (t_{water} , ϵ_{water}), where
 150 t is the travel time estimated for the measured trace. The volumetric water content θ is calculated according to the complex
 151 refractive index model (CRIM) following Roth et al. (1990) as:

$$\theta = \frac{\sqrt{\varepsilon} - \sqrt{\varepsilon_{soil}} - \phi(\sqrt{\varepsilon_{air}} - \sqrt{\varepsilon_{soil}})}{\sqrt{\varepsilon_{water}} - \sqrt{\varepsilon_{air}}} \quad (2)$$

152 where ϕ is the porosity which was calculated from the soil bulk density and ε_{soil} is set to 4.6. Fig. 4 shows the hourly time
153 series of soil water content. Characteristic differences in the soil water dynamics are evident for the distinct soil profiles and
154 depths to be attributed, e.g., to the differences in soil texture and soil layering or, locally to groundwater dynamics.

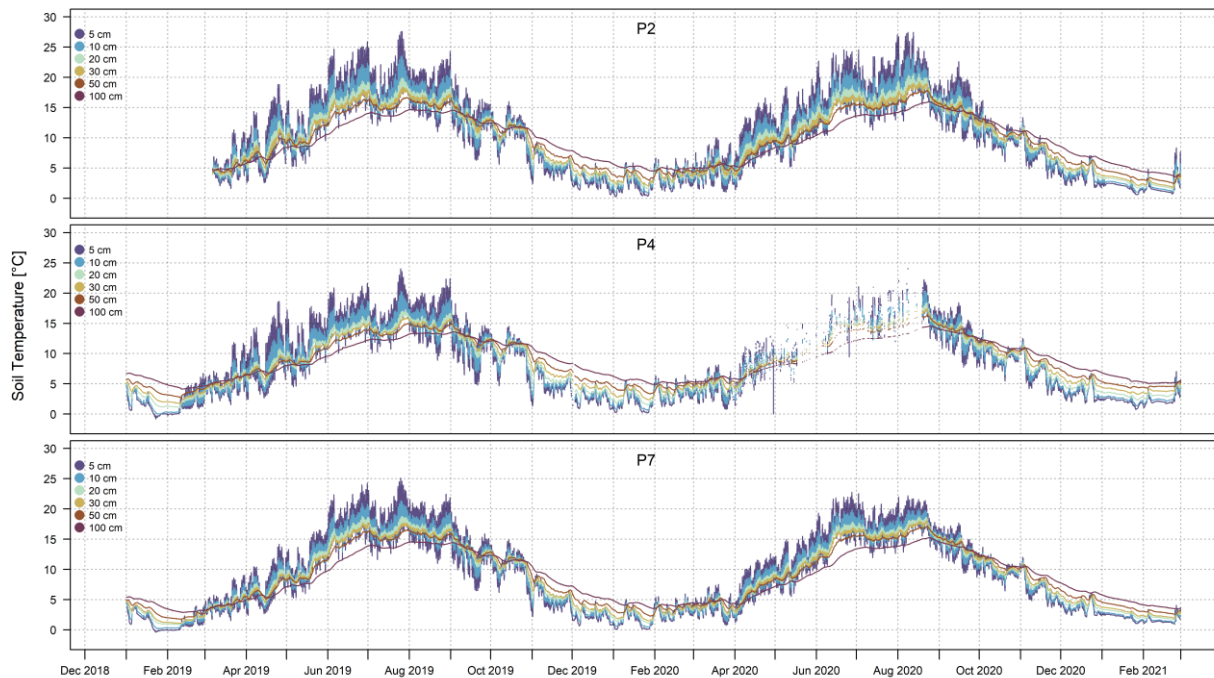


155

156 **Figure 4: Time series of soil water content data. The plots were made using the data set as it appears in the online archive. The data**
 157 **are plotted using a scientific colour scale from Crameri (2018) chosen according to the principles described in Crameri et al. (2020).**

158 3.2 Soil temperature

159 The stations P2, P4 and P7 are instrumented with one Th3-s soil temperature profile probe (formerly UMS GmbH, Munich,
160 Germany) each, located nearby the instrumented soil profiles (Fig. 2) and connected via SDI-12 to the same data loggers and
161 power supply. The probes consist of six temperature sensors cased inside a tube made of glass-fiber reinforced plastic and
162 placed at the fixed depths of 5, 10, 20, 30, 50 and 100 cm. Soil temperature is measured at the same times as the TDR traces.
163 The measured data are shown in Fig. 5. The influence of the geographical exposure of the slopes is particularly evident, e.g.
164 overall higher temperature and stronger dynamics for the south-exposed slopes compared to the other areas, as well as the
165 strongest dynamics near the surface compared to the deepest sensors. For every temperature profile, the soil temperature values
166 corresponding to the depths of the TDR profiles within the same cluster (i.e., the same topographic unit, namely Northern
167 slope, valley bottom and Southern slope) are calculated based on a linear interpolation and used for calculating the temperature
168 correction of the TDR measured soil water content values from the TDR traces according to Kaatzte (1989). By doing this, we
169 assume that i) the soil temperature changes linearly with depth between the observations at 5, 10, 20, 30, 50 and 100 cm,
170 regardless of material properties changes in-between, and ii) the soil temperature measured at each of the three plots (i.e., P2,
171 P4 and P7) is representative for the cluster (i.e., cluster North consisting of P1, P2 and P3, measured at P2; cluster Valley
172 consisting of P4 and P5, measured at P4; cluster South consisting of P6, P7 and P8, measured at P7).

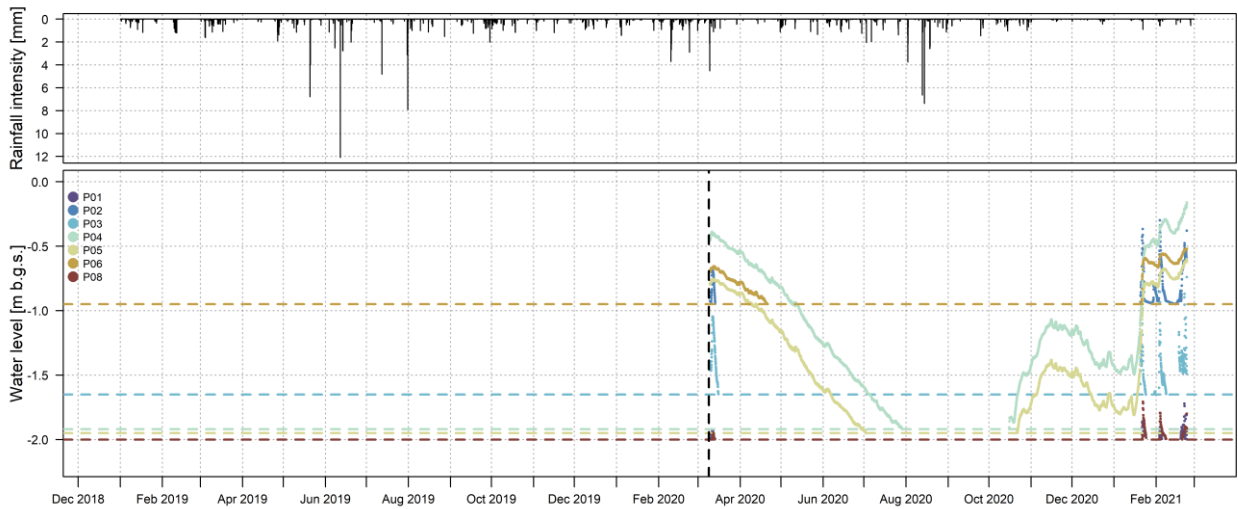


173

174 **Figure 5: Time series of soil temperature data. The plots were made using the data set as it appears in the online archive. The data**
175 **are plotted using a scientific colour scale from Crameri (2018) chosen according to the principles described in Crameri et al. (2020).**

176 3.3 Water level

177 Every station of the *STH-net* is equipped with a monitoring well consisting of a LDPE (i.e, low-density polyethylene) tube
178 drilled to the maximum depth of 2 m and instrumented with levelogger LTC (Solinst, Ontario, Canada), model 3001- M10.
179 Due to an initial malfunctioning of the sensors, only the data measured since March 9th, 2020 are available. In contrast to the
180 other measurements of the data set presented here, the water level data are downloaded manually. Figure 6 shows the time
181 series of the water level data and reports the maximum depth for every well. Seasonal dynamics of the groundwater level are
182 evident for the wells in the valley bottom (P4 and P5) and for P6, located next to the creek. The wells on the slopes (P1, P2,
183 P3, P7 and P8) stay dry for most of the monitored period and only show quick rises and recessions of the water level in the
184 winter and spring season.

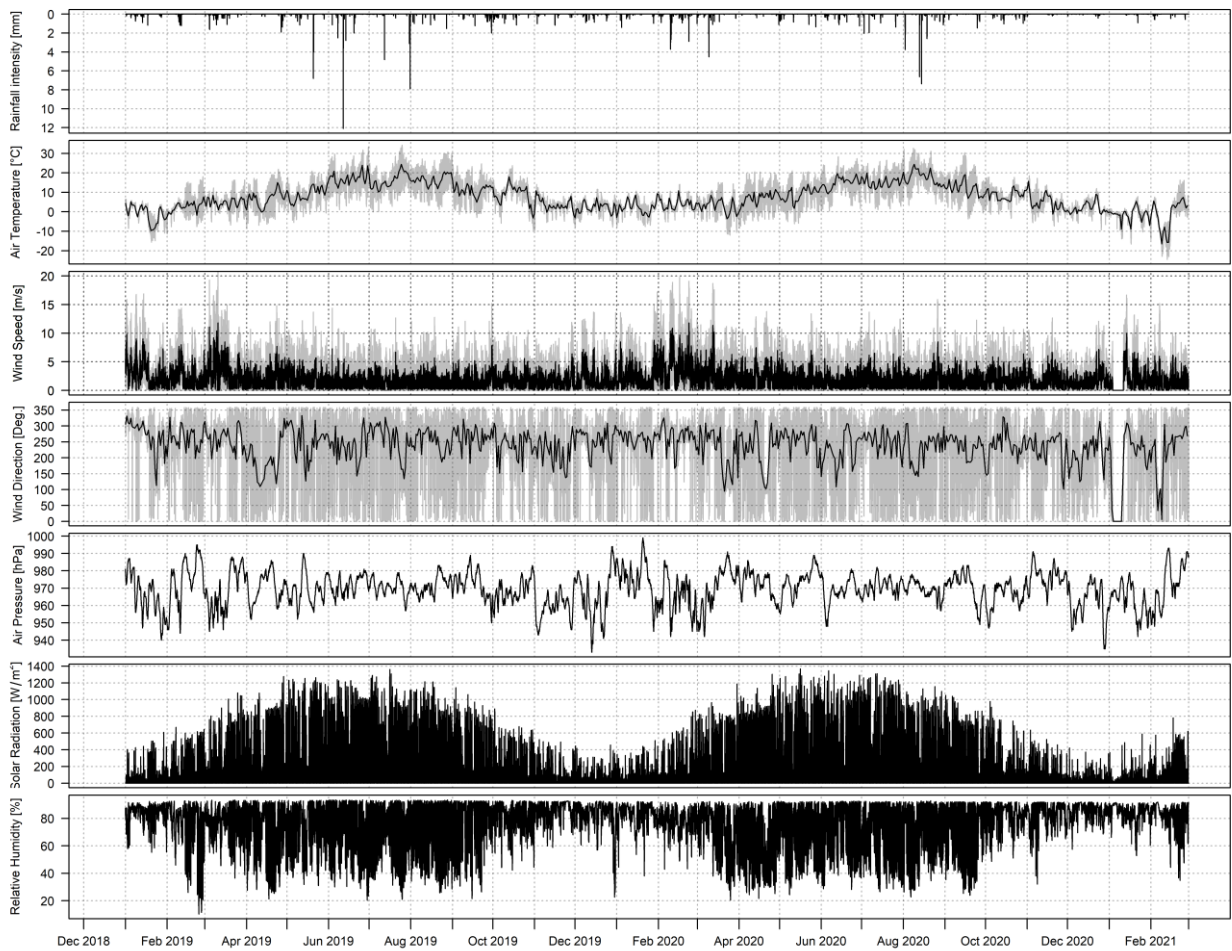


185

186 **Figure 6: Time series of water level data. The plots were made using the data set as it appears in the online archive. The dashed**
187 **vertical line indicates the start of the measurements (March 9th, 2020). The dashed horizontal lines indicate the depth of the wells.**
188 **The data are plotted using a scientific colour scale from Crameri (2018) chosen according to the principles described in Crameri et**
189 **al. (2020).**

190 3.4 Meteorological data

191 In the central part of the Schäfertal Hillslope site (Fig. 1), a WXT 520 weather station (Vaisala Oyj, Laskutus, Finland)
192 equipped with a CMP3-L pyranometer (Kipp & Zonen, Delft, Netherlands) installed at the height of 2 m measures the wind
193 vector, air temperature and pressure, relative humidity, liquid precipitation, hail and solar radiation. The system is fully
194 integrated with the data logger of the central monitoring station and the meteorological variables are measured at the same
195 times as the TDR and soil temperature profile probes. Fig. 7 shows the hourly time series of the meteorological variables.

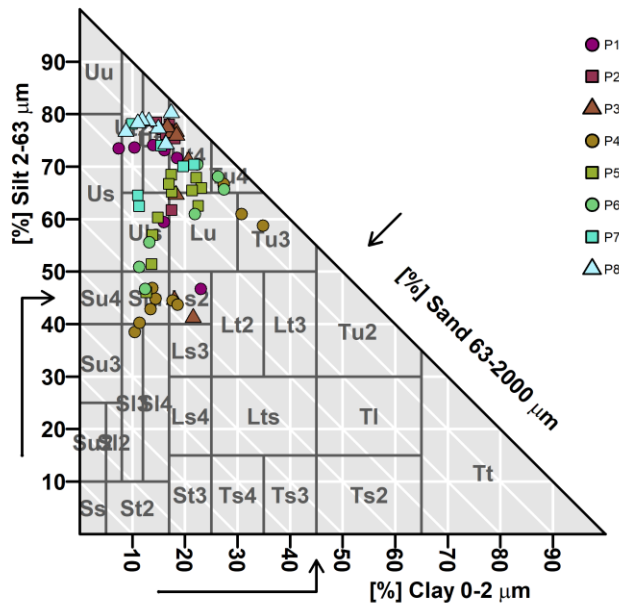


196

197 **Figure 7: Time series of all the meteorological variables measured at the *Schäfertal Hillslope* site. The plots were made using the**
 198 **data set as it appears in the online archive. The black line in the second, third and fourth plots shows the daily average temperature,**
 199 **the average wind speed and the daily average wind direction, respectively while all other data are in 10-min time steps.**

200 3.5 Soil properties

201 During the installation of the STH-net, one bulk soil sample and one volumetric soil sample were collected at every soil pit at
 202 the same depth as each of the TDR probes were installed. From the bulk samples, the percentage of sand, silt and clay in the
 203 fine earth fraction was determined in the laboratory using the pipette method. The volumetric soil samples were collected with
 204 a stainless stain ring and used for the soil porosity and bulk density estimation. Fig. 8 shows the classification of the soil
 205 samples according to the German soil textural classes (Ad-hoc-AG Boden, 2005), considered suitable for the soil
 206 parameterization for physically-based hydrological modelling (Bormann, 2007).



207

208 **Figure 8: Soil textural classification according to the German *Bodenkundliche Kartieranleitung* (Ad-hoc-AG Boden, 2005) grouped**
 209 **by soil profiles (P1 to P8). Ss: pure sand; Su2: slightly silty sand; Sl2: slightly loamy sand; Sl3: medium loamy sand; St2: slightly**
 210 **clayey sand; Su3: medium silty sand; Su4: highly silty sand; Slu: loamy silty sand; Sl4: highly loamy sand; St3: medium clayey sand;**
 211 **Ls2: slightly sandy loam Ls3: medium sandy loam; Ls4: highly sandy loam; Lt2: slightly clayey loam; Lts: clayey sandy loam; Ts4:**
 212 **highly sandy clay; Ts3: medium sandy clay; Uu: pure silt; Us: sandy silt; Ut2: slightly clayey silt; Ut3: medium clayey silt; Uls: loamy**
 213 **sandy silt; Ut4: highly clayey silt; Lu: silty loam; Lt3: medium clayey loam; Tu3: medium silty clay; Ts2: slightly sandy clay; Tu4:**
 214 **highly silty clay; Tu2: slightly silty clay; Tl: loamy clay; Tt: pure clay. The figure was created in RStudio with the package “The Soil**
 215 **Texture Wizard” (<https://CRAN.R-project.org/package=soiltexture>) by Julien Moeys. The data are plotted using a scientific colour**
 216 **scale from Crameri (2018) chosen according to the principles described in Crameri et al. (2020).**

217 4 Uncertainties and data usability

218 For the estimation of soil water content using a composite dielectric approach, some physical parameters must be known.
 219 These are primarily temperature, porosity and the dielectric number of the solid matrix (ϵ_{soil}). Among them, soil temperature
 220 plays the major role in determining the global uncertainty. As part of the *STH-net*, soil temperature is measured in situ at the
 221 same time as the TDR waveforms, which enables an accurate temperature correction. The soil porosity was estimated for every
 222 sampling point from undisturbed soil cores and introduces an uncertainty. For ϵ_{soil} we have chosen the value of 4.6,
 223 corresponding to the dielectric permittivity of quartz. This value was chosen arbitrarily hence introduces an uncertainty. For
 224 a more extensive discussion about the uncertainty of the soil water content estimation as due to the single parameters we refer
 225 to Roth et al. (1990). For the data set presented here, we estimated the uncertainty of the calculated soil water content using
 226 the CRIM formula by varying the values of ϵ_{soil} and porosity between 4 and 6 and between 0.3 and 0.5, respectively (similar

227 to Wollschläger et al., 2010). We obtained values $< \pm 0.03 \text{ m}^3/\text{m}^3$ as largest uncertainty of the soil water content estimation.
 228 This information is reported in Table 1 along with the measurement range, accuracy and resolution of the other variables
 229 provided within the data set described in this article.

230 Rain gauges may misestimate the rainfall rate under certain circumstances, especially when rainfall events are associated to
 231 strong wind. The experiment described in Basara et al. (2009) shows that a sensor similar to the one installed at the *Schäferfetal*
 232 *Hillslope* site overestimates the rainfall intensity in an urban environment. The rainfall rate data presented in this article were
 233 compared to those of several other rain gauges (data from partner research institute, not available here) located ca. 100 m away
 234 from the site. The rainfall intensity values measured by our sensor do not underestimate the rainfall rate values nor completely
 235 miss rainfall events. With our data set, we make the measured data available to any interested scientists along with all relevant
 236 site information and let them the choice about eventual compensation measures to be applied. The correction function proposed
 237 by Richter (1995) is commonly used for studies conducted in Central Germany to account for the possible wind-induced
 238 underestimation of the rainfall intensity.

239 Until a few years ago, the Schäferfetal catchment used to be affected by significant snowfall, with major snowmelt events
 240 occurring between January and April, whose effects on the hydrological processes are described, e.g., in Ollesch et al. (2005).
 241 In the last years, however, no significant snowfall events were observed. The last winter period (December 2020 to February
 242 2021), instead, was characterized by exceptionally intense snowfall (with a maximum of ca. 45 cm on February 8th, 2021) that
 243 accumulated and persisted. Unfortunately, the technical infrastructure currently available at the site does not allow a
 244 meaningful estimation of the snow height and distribution during the monitoring period, hence the snowfall events are not
 245 recorded by the weather station in use (see Fig. 7). Because of this, the snow contribution to the water balance needs to be
 246 derived from the meteorological and soil temperature data available.

247 Overall, 9.3 % of the soil water content data and 7.6 % of the soil temperature data are missing (particularly until March 2019
 248 for the station North and between April and August 2020 for the station Valley) due to various technical failures.

249 **Table 1: Measurement range, accuracy and resolution of the measurement devices described in Section 3.**

	Measurement range	Accuracy	Resolution
STH-net station			
Soil water content ¹	0 to 1 m^3/m^3	$< \pm 0.03 \text{ m}^3/\text{m}^3$	-
Soil temperature ²	-20°C to +50°C	$\pm 0,1^\circ\text{C}$	0,034°C
Water level ³	0 to 50°C (Barologger 5: -10 to +50°C), FS = 10 m	$\pm 0.5 \text{ cm}$	0.0006% FS
Weather station			
Barometric Pressure ⁴	600 to 1100 hPa	$\pm 0.5 \text{ hPa}$ at 0 to +30 °C $\pm 1 \text{ hPa}$ at -52 to +60 °C	0.1 hPa, 10 Pa, 0.001 bar, 0.1 mmHg, 0.01 inHg
Air Temperature ⁴	-52 to +60 °C	$\pm 0.3 \text{ }^\circ\text{C}$	0.1 °C
Wind speed ⁴	0 to 60 m/s	$\pm 3 \%$ at 10 m/s	0.1 m/s
Wind direction ⁴	0 to 360° azimuth	$\pm 3.0^\circ$	1°
Relative Humidity ⁴	0 to 100 % RH	$\pm 3 \%$ RH at 0 to 90 %RH	0.1 %RH

		±5 %RH at 90 to 100 %RH	
Rainfall intensity ⁴	0 to 200 mm/h (broader range with reduced accuracy)	Daily accumulation: better than 5 %, weather dependent	0.01 mm
Hail ⁴	n.a.	n.a	0.1 hit/cm ²
Solar radiation ⁵	Maximum solar irradiance: 2000 W/m ²	±5 %	< ±5 W/m ²

250 ¹ custom-made TDR probes (Helmholtz Centre for Environmental Research GmbH – UFZ, Leipzig, Germany)

251 ² Th3-s soil temperature profile probe (formerly UMS GmbH, Munich, Germany). Source:
 252 <https://www.google.com/url?sa=t&rct=j&q=&esrc=s&source=web&cd=&ved=2ahUKEwjQjpTu4bvAhWm4YUKHTKhCsUQFjABegQIARAC&url=http%3A%2F%2Fcnyhome.cafe24.com%2Fpdf%2FTh3sManual.pdf&usg=AOvVaw1JN8EI6XoJ6F3LyJw9PnnK> (accessed Apr 13th, 2021).

253 ³ 3001-M10 levellogger LTC (Solinst, Ontario, Canada). Source: <https://www.solinst.com/products/data/3001-ltc.pdf> (accessed
 254 Apr 13th, 2021).

255 ⁴ WXT 520 weather station (Vaisala Oyj, Laskutus, Finland). Source:
 256 <https://www.vaisala.com/en/file/9411/download?token=DOb1ETJK> (accessed Apr 13th, 2021).

257 ⁵ CMP3-L pyranometer (Kipp & Zonen, Delft, Netherlands). Source: <https://www.kippzonen.com/Product/11/CMP3-Pyranometer> (accessed Apr 13th, 2021).

261 5 Data management

262 The *STH-net* data stored by the three data loggers are accessed and downloaded remotely using the software *Loggernet*
 263 (Campbell Scientific Inc., Logan, UT, United States). The only exception are the water level data, which are manually
 264 downloaded. The data files are regularly quality checked and uploaded to the EUDAT record *STH-net*
 265 (<https://b2share.eudat.eu/records/82818db7be054f5eb921d386a0bcaa74>), where they remain available for download.

266 6 Data sets

267 The *STH-net* data are archived as separate text files for the different data types: soil water content, soil temperature, water level
 268 and meteorological variables. Furthermore, the geographic coordinates of the measurement locations and the soil information
 269 are available for download. The time series data start from January 1st, 2019 and continue with hourly time steps until the most
 270 recent update. At the time of the manuscript submission, the latest entry refers to February 28th, 2021. The water level data are
 271 available with a 2-hours resolution and covers the time period between March 6th, 2020 and February, 23rd, 2021. All the data
 272 published in the online archive (DOI 10.23728/b2share.82818db7be054f5eb921d386a0bcaa74) will be updated approximately
 273 on a 3-months basis.

274 **7 Data availability**

275 The *STH-net* data are available under a dynamic identifier DOI 10.23728/b2share.82818db7be054f5eb921d386a0bcaa74
276 (Martini et al., 2020) at the time of the manuscript submission (from there, all future versions of the archive can be easily
277 accessed) under the Creative Commons Attribution license (CC-BY 4.0).

278 **Author contribution**

279 Edoardo Martini: conceptualization, data curation, formal analysis, funding acquisition, investigation, methodology,
280 visualization, writing – original draft preparation, writing – review & editing.

281 Matteo Bauckholt: data curation.

282 Simon Kögler: conceptualization, data curation, methodology.

283 Manuel Kreck: data curation, methodology, writing – review & editing.

284 Kurt Roth: conceptualization, resources, writing – review & editing

285 Ulrike Werban: conceptualization, funding acquisition, resources, writing – review & editing

286 Ute Wollschläger: conceptualization, writing – review & editing

287 Steffen Zacharias: conceptualization, funding acquisition, resources, writing – review & editing

288 **Competing interests**

289 The authors declare that they have no conflict of interest.

290 **Acknowledgments**

291 The installation and operation of Schäfertal Hillslope site research infrastructure was funded and supported by the Terrestrial
292 Environmental Observatories (TERENO), which is a joint collaboration program involving several Helmholtz Research
293 Centres in Germany, and the TERENO observatory Harz/Central German Lowland operated by the UFZ Helmholtz Centre
294 for Environmental Research is gratefully acknowledged for providing access to the *Schäfertal Hillslope* site and to the *STH-*
295 *net* data. Edoardo Martini received funding from the German Research Foundation (DFG) through the research grant MA
296 7936/1-1.

297 **References**

298 Ad-hoc-Arbeitsgruppe Boden: Bodenkundliche Kartieranleitung, Bundesanstalt für Geowissenschaften und Rohstoffe in
299 Zusammenarbeit mit den Staatlichen Geologischen Diensten, 5. Aufl., 438p., Hannover, ISBN 978-3-510-95920-4, 2005.

300 Bauser, H.H., Jaumann, S., Berg, D., and Roth, K.: EnKF with closed-eye period - Towards a consistent aggregation of
301 information in soil hydrology, *Hydrol. Earth Syst. Sci.*, 20, 4999–5014. <https://doi.org/10.5194/hess-20-4999-2016>, 2016.

302 Bauser, H.H., Riedel, L., Berg, D., Troch, P.A., and Roth, K.: Challenges with effective representations of heterogeneity in
303 soil hydrology based on local water content measurements. *Vadose Zone Journal*, 19:e20040,
304 <https://doi.org/10.1002/vzj2.20040>, 2020.

305 Blöschl, G., Bierkens, M. F. P., Chambel, A., et al.: Twenty-three Unsolved Problems in Hydrology (UPH) – a community
306 perspective, *Hydrolog. Sci. J.*, 64, 1141–1158, <https://doi.org/10.1080/02626667.2019.1620507>, 2019.

307 Borchardt, D.: Geoökologische Erkundung und hydrologische Analyse von Kleinzugsgebieten des unteren
308 Mittelgebirgsbereichs, dargestellt am Beispiel der oberen Selke, Harz, *Petermanns Geogr. Mitteil.*, 82, 251–262, 1982.

309 Botto, A., Belluco, E., and Camporese, M.: Multi-source data assimilation for physically based hydrological modeling of an
310 experimental hillslope, *Hydrol. Earth Syst. Sci.*, 22, 4251–4266, <https://doi.org/10.5194/hess-22-4251-2018>, 2018.

311 Bormann, H.: Analysis of the suitability of the German soil texture classification for the regional scale application of physical
312 based hydrological model, *Adv. Geosci.*, 11, 7–13, <https://doi.org/10.5194/adgeo-11-7-2007>, 2007.

313 Bronstert, A.: Capabilities and limitations of detailed hillslope hydrological modelling, *Hydrol. Process.*, 13: 21-48.
314 [doi:10.1002/\(SICI\)1099-1085\(199901\)13:1<21::AID-HYP702>3.0.CO;2-4](https://doi.org/10.1002/(SICI)1099-1085(199901)13:1<21::AID-HYP702>3.0.CO;2-4), 1999.

315 Clark, M.P., Bierkens, M.F.P., Samaniego, L., Woods, R.A., Uijlenhoet, R., Bennett, K.E., Pauwels, V.R.N., Cai, X., Wood,
316 A.W., and Peters-Lidard, C.D.: The evolution of process-based hydrologic models: historical challenges and the collective
317 quest for physical realism, *Hydrol. Earth Syst. Sci.*, 21, 3427-3440, <https://doi.org/10.5194/hess-21-3427-2017>, 2017.

318 Crameri, F.: Scientific colour maps, *Zenodo*, <http://doi.org/10.5281/zenodo.1243862>, 2018.

319 Crameri, F., Shephard, G.E., and Heron, P.J.: The misuse of colour in science communication, *Nature Communications*, 11,
320 5444, [doi:10.1038/s41467-020-19160-7](https://doi.org/10.1038/s41467-020-19160-7), 2020.

321 Fan, Y., Clark, M., Lawrence, D. M., Swenson, S., Band, L. E., Brantley, S. L., et al.: Hillslope hydrology in global change
322 research and Earth system modeling, *Water Resources Research*, 55, 1737–1772, <https://doi.org/10.1029/2018WR023903>,
323 2019.

324 Graeff, T., Zehe, E., Reusser, D., Lück, E., Schröder, B., Wenk, G., John, H., and Bronstert, A.: Process identification through
325 rejection of model structures in a mid-mountainous rural catchment: observations of rainfall–runoff response, geophysical
326 conditions and model inter-comparison, *Hydrol. Process.*, 23: 702-718. [doi:10.1002/hyp.7171](https://doi.org/10.1002/hyp.7171), 2009.

327 Kaatze, U.: Complex permittivity of water as a function of frequency and temperature, *J. Chem. Eng. Data* 1989, 34, 4, 371–
328 374, <https://doi.org/10.1021/je00058a001>, 1989.

329 IUSS Working Group WRB: World Reference Base for Soil Resources 2014, Update 2015. *World Soil Resources Reports*
330 106, FAO, Rome. ISBN 978-92-5-108369-7, 2015.

331 Martini, E., Wollschläger, U., Kögler, S., Behrens, T., Dietrich, P., Reinstorf, F., Schmidt, K., Weiler, M., Werban, U., and
332 Zacharias, S.: Spatial and temporal dynamics of hillslope-scale soil moisture patterns: characteristic states and transition
333 mechanisms, *Vadose Zone J.*, 14, [doi:10.2136/vzj2014.10.0150](https://doi.org/10.2136/vzj2014.10.0150), 2015.

334 Martini, E., Werban, U., Zacharias, S., Pohle, M., Dietrich, P., and Wollschläger, U.: Repeated electromagnetic induction
335 measurements for mapping soil moisture at the field scale: validation with data from a wireless soil moisture monitoring
336 network, *Hydrol. Earth Syst. Sci.*, 21, 495–513, <https://doi.org/10.5194/hess-21-495-2017>, 2017.

337 Martini, E., Wollschläger, U., Musolff, A., Werban, U., and Zacharias, S.: Principal component analysis of the spatiotemporal
338 pattern of soil moisture and apparent electrical conductivity, *Vadose Zone J.*, 16(10), doi:10.2136/vzj2016.12.0129, 2017.

339 Martini, E., Kögler, S., Kreck, M., Werban, U., Wollschläger, U., Zacharias, S.: STH-net, EUDAT,
340 <https://b2share.eudat.eu/records/82818db7be054f5eb921d386a0bcaa74>, 2020.

341 Ollesch, G., Sukhanovski, Y., Kistner, I., Rode, M., and Meissner, R.: Characterization and modelling of the spatial
342 heterogeneity of snowmelt erosion, *Earth Surf. Proc. Land.*, 30, 197–211, doi:10.1002/esp.1175, 2005.

343 Reinstorf, F.: Schäfertal, Harz Mountains, Germany. Poster, in: Status and Perspectives of Hydrology in Small Basins, Results
344 and recommendations of the International Workshop in Goslar-Hahnenklee, Germany 2009, and Inventory of Small
345 Hydrological Research Basins, 30 March–2 April 2009, Goslar-Hahnenklee, Germany, edited by: Schumann, S., Schmalz,
346 B., Meesenburg, H., and Schröder, U., available at:
347 [https://www.google.com/url?sa=t&rct=j&q=&esrc=s&source=web&cd=&ved=2ahUKEwjQluqSIMjsAhUOecAKHTnICqsQFjAAegQIAhAC&url=https%3A%2F%2Fwaterandchange.org%2Fwp-](https://www.google.com/url?sa=t&rct=j&q=&esrc=s&source=web&cd=&ved=2ahUKEwjQluqSIMjsAhUOecAKHTnICqsQFjAAegQIAhAC&url=https%3A%2F%2Fwaterandchange.org%2Fwp-content%2Fuploads%2F2017%2F04%2FHeft10_en.pdf&usg=AOvVaw2o4w_VX74jGiquRs3KaYVR)
348 [content%2Fuploads%2F2017%2F04%2FHeft10_en.pdf&usg=AOvVaw2o4w_VX74jGiquRs3KaYVR](https://www.google.com/url?sa=t&rct=j&q=&esrc=s&source=web&cd=&ved=2ahUKEwjQluqSIMjsAhUOecAKHTnICqsQFjAAegQIAhAC&url=https%3A%2F%2Fwaterandchange.org%2Fwp-content%2Fuploads%2F2017%2F04%2FHeft10_en.pdf&usg=AOvVaw2o4w_VX74jGiquRs3KaYVR) (last access: 22
349 October 2020), 2010.

351 Richter, D.: Ergebnisse methodischer Untersuchungen zur Korrektur des systematischen Meßfehlers des Hellmann-
352 Niederschlagsmessers, *Berichte des Deutschen Wetterdienstes* 194, Deutscher Wetterdienst, Offenbach am Main, ISBN:
353 3881483098, <http://nbn-resolving.de/urn:nbn:de:101:1-201601274368>, in German, 1995

354 Roth, K., Schulin, R., Flühler, H., and Attinger, W.: Calibration of time domain reflectometry for water content measurement
355 using a composite dielectric approach, *Water Resour. Res.*, 26, 2267–2273, doi:10.1029/WR026i010p02267, 1990.

356 RStudio Team: RStudio: Integrated Development for R. RStudio, Inc., Boston, MA URL <http://www.rstudio.com/>, 2019.

357 Schröter, I., Paasche, H., Dietrich, P., and Wollschläger, U.: Estimation of catchment-scale soil moisture patterns based on
358 terrain data and sparse TDR measurements using a Fuzzy C-Means clustering approach, *Vadose Zone J.*, 14,
359 doi:10.2136/vzj2015.01.0008, 2015.

360 United Nations: World Soil Day and International Year of Soils: A/RES/68/232, 2014.

361 Vogel, H.-J.: Scale issues in soil hydrology, *Vadose Zone J.*, 18(1). <https://doi.org/10.2136/vzj2019.01.0001>, 2019.

362 Vrugt, J.A., Stauffer, P.H., Wöhling, T., Robinson, B.A., and Vesselinov, V.V.: Inverse modeling of subsurface flow and
363 transport properties: A review with new developments, *Vadose Zone Journal*, 7, 843–864.
364 <https://doi.org/10.2136/vzj2007.0078>, 2008.

365 Vereecken, H., Huisman, J. A., Hendricks Franssen, H. J., Brüggemann, N., Bogaen, H. R., Kollet, S., Javaux, M., van der
366 Kruk, J., and Vanderborght, J.: Soil hydrology: Recent methodological advances, challenges, and perspectives. *Water*
367 *Resources Research*, <https://doi.org/10.1002/2014WR016852>, 2015.

368 Vereecken, H., Schnepf, A., Hopmans, J. W., Javaux, M., Or, D., Roose, T., J. Vanderborght, Young, M. H., Amelung, W.,
369 Aitkenhead, M., Allison, S. D., Assouline, S., Baveye, P., Berli, M., Brüggemann, N., Finke, P., Flury, M., Gaiser, T., Govers,
370 G., Ghezzehei, T., Hallett, P., Hendricks Franssen, H. J., Heppell, J., Horn, J., Huisman, J. A., Jacques, D., Jonard, F., Kollet,
371 S., Lafolie, F., Lamorski, K., Leitner, D., McBratney, A., Minasny, B., Montzka, C., Nowak, W., Pachepsky, Y., Padarian,
372 J., Romano, N., Roth, K., Rothfuss, Y., Rowe, E. C., Schwen, A., Šimůnek, J., Tiktak, A., van Dam, J., van der Zee, S. E. A.
373 T. M., Vogel, H.-J., Vrugt, J. A., Wöhling, T., & Young, I. M. (2016). Modeling Soil Processes: Review, Key challenges
374 and New Perspectives. *Vadose Zone Journal*, 15(5), 1–57, <https://doi.org/10.2136/vzj2015.09.0131>.

375 Wollschläger, U., Pfaff, T., and Roth, K.: Field-scale apparent hydraulic parameterisation obtained from TDR time series and
376 inverse modelling, *Hydrol. Earth Syst. Sci.*, 13, 1953-1966, doi:10.5194/hess-13-1953-2009, 2009.

377 Wollschläger, U., Gerhards, H., Yu, Q., and Roth, K.: Multi-channel ground-penetrating radar to explore spatial variations in
378 thaw depth and moisture content in the active layer of a permafrost site, *The Cryosphere* 4.3: 269-283, 2010.

379 Wollschläger, U., Attinger, S., Borchardt, D., Brauns, M., Cuntz, M., Dietrich, P., Fleckenstein, J.H., Friese, K., Friesen, J.,
380 Harpke, A., Hildebrandt, A., Jäckel, G., Kamjunke, N., Knöller, K., Kögler, S., Kolditz, O., Krieg, R., Kumar, R., Lausch,
381 A., Liess, M., Marx, A., Merz, R., Mueller, C., Musolff, A., Norf, H., Oswald, S.E., Rebmann, C., Reinstorf, F., Rode, M.,
382 Rink, K., Rinke, K., Samaniego, L., Vieweg, M., Vogel, H.-J., Weitere, M., Werban, U., Zink, M., and Zacharias, S. : The
383 Bode Hydrological Observatory: A platform for integrated, interdisciplinary hydro-ecological research within the TERENO
384 Harz/Central German Lowland Observatory, *Env. Earth Sci.*, 76:29, doi:10.1007/s12665-016-6327-5, 2017.

385 Zacharias, S., Bogena, H., Samaniego, L., Mauder, M., Fuß, R., Pütz, T., Frenzel, M., Schwank, M., Baessler, C., Butterbach-
386 Bahl, K., Bens, O., Borg, E., Brauer, A., Dietrich, P., Hajnsek, I., Helle, G., Kiese, R., Kunstmann, H., Klotz, S., Munch, J.
387 C., Papen, H., Priesack, E., Schmid, H. P., Steinbrecher, R., Rosenbaum, U., Teutsch, G., and Vereecken, H.: A network of
388 terrestrial environmental observatories in Germany, *Vadose Zone J.*, 10, 955–973, doi:10.2136/vzj2010.0139, 2011.

389